

See discussions, stats, and author profiles for this publication at: <https://www.researchgate.net/publication/224586513>

# Optical Flow from Motion Blurred Color Images

Conference Paper · June 2009

DOI: 10.1109/CRV.2009.15 · Source: IEEE Xplore

---

CITATIONS

5

READS

1,098

---

3 authors, including:



Milena Scaccia

McGill University

5 PUBLICATIONS 30 CITATIONS

[SEE PROFILE](#)



Ioannis M. Rekleitis

University of South Carolina

153 PUBLICATIONS 3,846 CITATIONS

[SEE PROFILE](#)

Some of the authors of this publication are also working on these related projects:



Visual Perception of Three-Dimensional (3-D) Cluttered Scenes [View project](#)



Exploration [View project](#)

# Optical Flow from Motion Blurred Color Images

Yasmina Schoueri Milena Scaccia

Ioannis Rekleitis

School of Computer Science, McGill University

[yasyas, yiannis]@cim.mcgill.ca, milena.scaccia@mail.mcgill.ca

## Abstract

*This paper presents an algorithm for the estimation of optical flow from a single, motion-blurred, color image. The proposed algorithm is based on earlier work that estimated the optical flow using the information from a single grey scale image. By treating the three color channels separately we improved the robustness of our approach. Since first introduced, different groups have used similar techniques of the original algorithm to estimate motion in a variety of applications. Experimental results from natural as well as artificially motion-blurred images are presented.*

## 1 Introduction

In a scene observed by a camera, motion blur may be produced from a combination of the movement of the camera and of the independent motion of the objects in the scene. In many cases, motion blur is regarded as undesirable noise that is to be removed to render a clearer image of the observed scene. Despite being regarded as a nuisance to the photographer, studies have shown that motion blur in an image has some practical interest in one of the fundamental problems of computer vision —the measurement of the apparent motion in an image, referred to as optical flow.

Estimating the motion blur parameters is useful for two different reasons. First, having an accurate estimate of the blurring parameters, image restoration in the form of deblurring can be achieved [9]. Second, by calculating the optical flow from a single motion blurred image, motion parameters for separate objects in the scene as well as egomotion can be inferred.

Different applications have been suggested to benefit from the motion blur estimation. Traffic cameras can infer the speed of passing vehicles using only the motion blur, thus avoiding detectable active sensing, such as radar. The motion blurred images can further be cleaned up to provide evidence in the form of licence plate numbers.

A methodology for the detection and subsequent correc-



**Figure 1. Motion blurred image.**

tion of the above mentioned blur is also of interest at the consumer level. This is due to the proliferation of digital and cell-phone cameras and their use, which often results in motion blurred photos in badly lit areas. Another application, linked to the availability of cell phone cameras, is the digital recording of business cards [18].

The next section discusses related work. Section 3 presents a brief overview of the effect of motion blur on images. In particular we discuss how motion blur appears in the frequency domain. Our approach is described in Section 4. A short description of the grey scale algorithm is discussed together with our extension to color images. Experimental results are then presented in Section 5. In the last section, we present conclusions and discuss future work.

## 2 Related work

The problem of estimating motion in a scene has received a lot of attention due to its broad application. The application of optical flow methods includes not only the problem of inferring the apparent motion of an observer and objects in the scene, but that of inferring the structure of the objects and their corresponding environment [2]. This was shown to have practical interest in image segmentation [16], surface structure reconstruction, inference of egomotion and active navigation [11], all of which require the optical flow as input information.

To date, various methods for computing the optical flow

have been proposed, the most widely used being differential methods. The first global differential method, introduced in 1980 by Horn and Schunck, consists of optimizing a function based on residuals from the brightness constancy constraint and a regularization term expressing the expected smoothness of the flow field [12]. There have been many extensions of this method, mainly varying the constraints used to solve the problem.

Global differential techniques have the advantage of yielding dense flow fields, yet are not as robust to noise as are local approaches such as the Lucas-Kanade method [15] which regards image patches and an affine model for the flow field. There have since been studies evaluating hybrid approaches that attempt to combine the main advantages of global and local approaches [3].

A drawback to the above mentioned traditional algorithms is that optical flow is calculated using a series of consecutive images under the assumption that pixels keep their brightness from one frame to the other, having changed their position only. That is, it is assumed that each image is taken with an infinitely small exposure time. Thus blurring due to motion within a frame is disregarded or treated as an additional source of noise.

Instead of being considered a degradation that is to be removed using one of the many deblurring methods developed [1], it has been shown that motion blur in an image may have some practical interest in fundamental computer vision problems, such as in the measurement of the optical flow [19].

In 1981, a series of psychophysical studies suggested that the human visual system [10] is able to process information about motion blur in order to infer information about objects in the scene. This has motivated the development of algorithms that take advantage of information encoded in the motion blur. This motivation, in conjunction with the use of a deblurring mechanism to distinguish features in a specific image, gave rise to a novel approach for obtaining information about motion in an image.

In 1995, an algorithm for extracting the parameters of motion blur in a single image in order to compute the optical flow was presented by Rekleitis. His approach relies heavily on the information present in the frequency domain. In particular, it exploits the key observation that motion blur introduces a ripple in the Fourier transform [19], from which we may extract information about the magnitude and orientation of the velocity vector given an image patch. This algorithm can be used in a stand-alone manner or to complement previous algorithms to address the issue of motion blur in a sequence of frames instead of merely ignoring it.

There has since been research that builds on the ideas of using information from motion blur. In 1996, Chen et al. presented a computational model that attempts to emulate the behavior of the human visual system in order to use it

in machine vision systems [5]. Further research on the human visual system carried out in 1999 by Geisler explores another potential neural mechanism for resolving motion orientation, which uses a spatial signal known as “motion streak” created by a fast enough moving localized image feature [8].

Aside from in-depth studies of the human visual system, other methods for identifying motion blur parameters from a single blurred image have been developed. In 1997, Yitzhaky and Kopeika developed a method for characterizing the point spread function of the blur. Their identification method bases itself on the concept that image characteristics along the direction of motion are different from characteristics in other directions [20].

There has also been research examining the usefulness and limitations of Rekleitis’ approach of estimating blur parameters, which has been adapted in 2005 by Qi et al. to enhance optical character recognition (OCR) in blurred text. Rekleitis’ algorithm has been shown to work for most blur orientations and extents. However the average error estimation of blur extent was shown to be quite large, not making it suitable for OCR. Qi et al. thus adopt a different thresholding technique in blur orientation estimation and further estimate motion parameters due to uniform acceleration [18].

The use of motion blur has also had an increasing number of applications in areas such as real-time ball-tracking systems in live sports programs [7], in vehicle speed detection [14], in object depth recovery [4], as well as in the estimation of motion for a tracking vision system [13].

### 3 Motion Blur

As mentioned previously, most motion estimation algorithms infer optical flow by considering a sequence of images. In addition, they assume that pixels maintain their brightness in subsequent frames, their positions being the only thing that changes. That is, they assume that each image is acquired with a very small exposure time. But if this does not happen to be the case, then with a somewhat large exposure time, different points traveling in the scene cause their corresponding projections on the image plane to affect several pixels. Hence in the capturing of any single point, a number of scene points get projected onto the image plane during the time of exposure, each of them contributing to the final color and brightness of the image point.

More formally, the motion blur can be described as the effect of applying the linear filter:

$$\mathbf{B}(x, y) = \mathbf{I}(x, y) * h(x, y) \quad (1)$$

where  $\mathbf{B}$  is the blurred image,  $\mathbf{I}$  is the image taken with exposure time  $T_e = 0$ , and  $h$  is the convolution kernel:

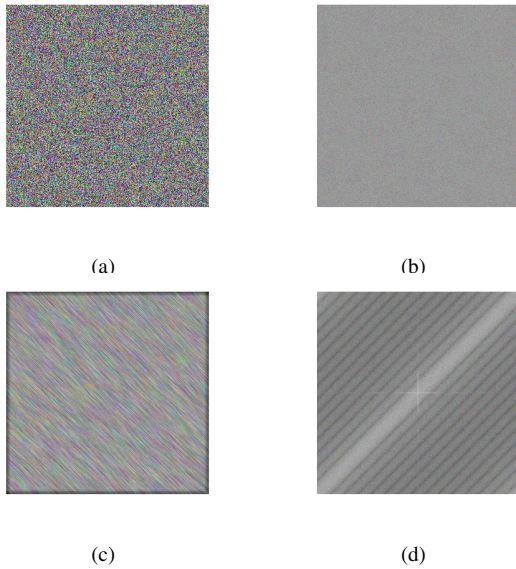


**Figure 2. (a) A color Image of random noise. (b) The power spectrum of (a). (c) The same image affected by an artificial motion blur. (d) The power spectrum of the motion blurred image.**

$$h(x, y) = \begin{cases} \frac{1}{d}, & 0 \leq |x| \leq d \cos(\alpha) \quad y = d \sin(\alpha) \\ 0, & \text{otherwise} \end{cases} \quad (2)$$

where  $\alpha$  is the angle of the motion that caused the blur, and  $d = V_o T_e$  is the number of scene points that affect a specific pixel. Given the convolution kernel, we can also produce artificially blurred images, which can serve as ground truth to test our approach.

In the frequency domain the convolution described in Eq. 1 results in the multiplication of the Fourier transform of image  $I$  times the Fourier transform of the convolution kernel  $h$ . It has been shown [19] that one prominent characteristic of the convolution kernel in the frequency domain is a ripple that extends perpendicular to the direction of the blur; cf. Fig. 2d. This ripple is thus used to detect the direction of the blur. In the most favorable case the observed scene consists of random noise, as in Fig. 2a. In that case the Fourier of the non-blurred image has no prominent structure, cf. Fig. 2b, and the detection of the optical flow is very easy. Clearly when there is structure in the scene, the optical flow detection is more challenging. The following section presents an outline of the proposed algorithm.

## 4 Optical Flow Estimation

In order to apply our algorithm to color images we treat the three color channels (red, green, and blue) as individual grey scale images. The optical flow is estimated in each

color channel using the algorithm proposed in [19] and the results are combined to form the final optical flow estimates.

### 4.1 Windowing and Zero-Padding

A significant source of error is the well studied ringing effect. When we take the Fourier transform of an image patch, the abrupt transition results in artifacts in the frequency domain. To mitigate the ringing effect, each image patch is masked using a 2D Gaussian function. Then, to increase the frequency resolution of the Fourier transform, the masked image patch, originally of size  $N$ , is zero-padded to size  $2N$ . However, if the patch pixel values are much larger, the blur is then harder to detect, thus the difference between the pixel value and the mean of the patch is zero-padded instead [17].

### 4.2 Orientation Estimation

As seen earlier, the power spectrum of the blurred image is characterized by a central ripple that goes across the direction of the motion. In order to extract this orientation we treat the power spectra as an image and a linear filter is applied in order to identify the orientation of the ripple. More specifically the second derivative of a two dimensional Gaussian is used. The second derivative of the Gaussian along the x-axis is  $G_2^0 = \frac{\partial^2 G}{\partial x^2}$ . In order to extract the orientation of the ripple, we have to find the angle  $\theta$  for which the response of the second derivative of a Gaussian filter – oriented at that angle ( $G_2^\theta$ ) – is maximum. Fortunately, the second derivative of the Gaussian  $G_2^\theta$  belongs to a family of filters called “steerable filters” [6], whose response can be calculate at any angle  $\theta$  based only on the responses of three *basis filters*.

The response of the second derivative of the Gaussian at an angle  $\theta$  ( $RG_2^\theta$ ) is given in equation 3. The set of the three basis filters is shown in the left column of the table 1 and in the right column we could see the three *interpolation functions* that are used.

$$RG_2^\theta = k_a(\theta)RG_{2a} + k_b(\theta)RG_{2b} + k_c(\theta)RG_{2c} \quad (3)$$

### 4.3 Cepstral Analysis

If only one line of the blurred image is taken (across the direction of the motion) then the blurred signal is equivalent to the convolution of the unblurred signal by the step function which in the frequency domain is transformed into the sinc function ( $\text{sinc}(x) = \frac{\sin x}{x}$ ). The period of the sinc pulse is equivalent to the length of the step function, which is in turn equivalent to the velocity magnitude. If we take the Fourier transform of the sinc function, its period appears

|                                 |  |
|---------------------------------|--|
| $G_{2a} = 0.921(2x^2 - 1)e^\mu$ | $k_a(\theta) = \cos^2(\theta)$             |
| $G_{2b} = 1.843xye^\mu$         | $k_b(\theta) = -2\cos(\theta)\sin(\theta)$ |
| $G_{2c} = 0.921(2y^2 - 1)e^\mu$ | $k_c(\theta) = \sin^2(\theta)$             |
| $\mu = -(x^2 + y^2)$            |  |

**Table 1. The three basis filters and their interpolation functions**

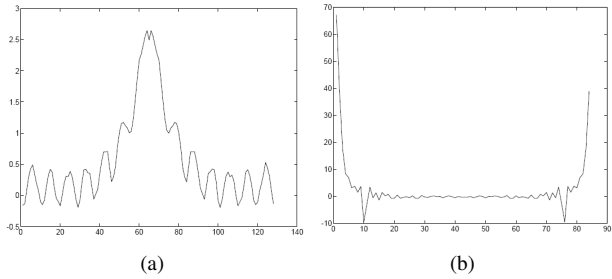


**Figure 3. (a) The collapsed power spectrum of Fig. 2d. (b) The power spectrum of the collapsed power spectrum.**

as a negative peak. To improve robustness, we compute the magnitude of the velocity by using a 1D projection of the power spectra onto the line across the velocity vector orientation that passes through the origin.

To approximate the 1D signal, the power spectra is collapsed from 2D into 1D. The resulting signal also takes on the shape of the sinc function, because the ripple caused by the motion blur is the dominant feature; cf. Fig. 2d. Every pixel  $P(x,y)$  in the power spectra is mapped into the line that passes through the origin  $O$  at an angle  $\theta$  with the x-axis equal to the orientation of the motion, and at distance  $d = x\cos(\theta) + y\sin(\theta)$ . The Fourier transform of the sinc function is almost identical in shape to the one that appears when we take the Fourier transform of the collapsed spectrum cf. Fig. 3a,b.

#### 4.4 Color Image Optical Flow Estimation

The results from the three color channels are combined as a weighted sum. Currently, there is a binary decision to select if a channel contributes based on the response of the steerable filters. If the difference between the maximum and the minimum response of the steerable filter is not significant, then the flow estimate from that channel for the specific location is not considered. All the estimates that are above a threshold then are weighted equally.

## 5 Experimental Results

The proposed algorithm was tested in a variety of synthetic and naturally blurred images. The first results presented show the effect of using two different motions along the red and the green channels. A random dot image was used in order to maximize the effect of the motion blur. If the response of the steerable filter was found to be non-significant for a pixel, then its flow vector was not displayed in the flow map. Figure 4a shows the color blurred image. Distinct directions of motion are clear, vertical in the red channel, and horizontal in the green channel. Figure 4b presents a grey scale version of the same image; and Fig. 4c presents the optical flow estimated from the grey scale image. As expected no significant motion was detected. Figures 4d-f contains the optical flow estimated in the three color channels. Distinct motion was detected along the direction of blur for the red and green channels. Although this example presented a most favorable case, it showcases the importance of detecting motion blur along different colors.

The next experiments used natural images that were blurred due to camera motion. The first image was taken from the back of a moving train; cf. Fig. 5. The area between the train tracks closer to the camera was moving the fastest and thus was the most blurred. As can be seen from the estimates using the three color channels Fig. 5a-c in several positions there was no estimate. By using a weighted sum of the estimates we were able to recover most of the optical flow; cf. Fig. 5d.

The second photograph was taken by panning the camera following the motion of a group of bicycle riders; cf. Fig. 5. Due to the camera motion the background was uniformly blurred while the bicycles and their drivers are not. It is worth noting that the wheels of the bicycles were more blurred and this was estimated by our approach. Due to the size of the sub-window used, some of these contained more than one motion. Figure 5a-c show the optical flow calculations from three color channels; while Fig. 5d presents the cumulative results.

## 6 Conclusions

From the qualitative results presented above, the optical flow was successfully estimated using a single blurred image instead of the traditional sequence of images. The proposed algorithm can be used in a stand-alone manner or can be used to complement previous algorithms. The original algorithm was extended to work with color images taking advantage of the often redundant information that exist in the three color channels.

One possible future direction is to employ the different flow estimates for different colored objects as an additional clue to object detection.

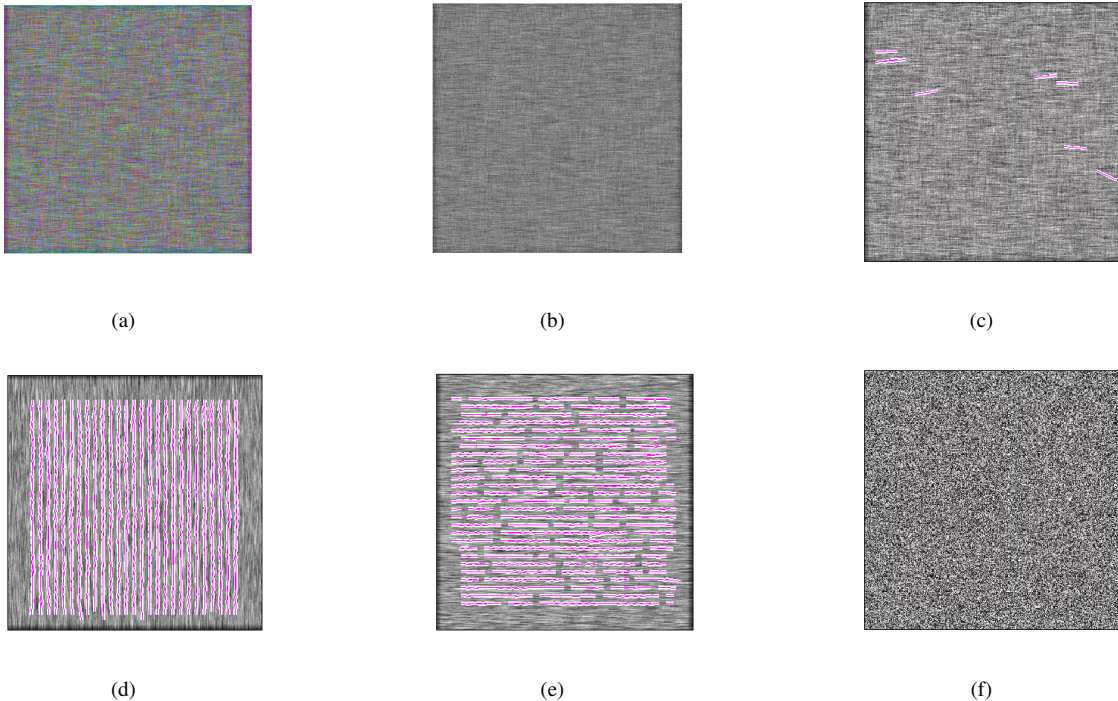


**Figure 4.** (a) A color image artificially blurred. (b) Grey scale representation of (a). (c) The optical flow estimated from the grey scale image. (d) Optical flow from red channel. (e) Optical flow from green channel. (f) Optical flow from blue channel.

With regard to extending the algorithm to work with RGB images, we have a few open questions at hand. Because we end up with three different optical flow maps as a result of applying the original algorithm to the three channels, this allows us to detect different motion directions. We ask the question as to whether different objects can become segmented according to their color channel and whether this leads to applications in object detection.

Another interesting problem would be to investigate the effect of different color spaces in the optical flow estimation. For example using the YUV or HSV color spaces as opposed to RGB. Perhaps this would give us a different perspective on the effect of color, and may or may not be used in conjunction with the RGB results in order to facilitate the detection of objects according to their color channels.

Chromatic aberrations in digital images is another area where the proposed technique can find applications. As the different channels are affected differently, the optical flow estimates could potentially identify the discrepancy and improve end results.

Other goals include completing the process of filtering outliers. We have yet to determine whether carrying out the filtering before or after combining the flow maps will yield more accurate results, if at all.

## References

- [1] M. Ben-Ezra and S. Nayer. Motion-based motion deblurring. *IEEE Trans. on Pattern Analysis and Machine Intelligence*, 26:689–698, 2004.
- [2] C. Brown. *Advances in Computer Vision*. Lawrence Erlbaum, 1987.
- [3] A. Bruhn, J. Weickert, and C. Schnrr. Image motion estimation from motion smear - a new computational model. *Int. Journal of Computer Vision*, 61(3):211–231, March 2005.
- [4] C. Chang. Speed and depth measurements from motion blurred images. Master's thesis, National Chung Cheng University, 2006.
- [5] W. Chen and N. Nandhakuman. Image motion estimation from motion smear - a new computational model. *IEEE Trans. on Pattern Analysis and Machine Intelligence*, 18(4):412–425, April 1996.
- [6] W. T. Freeman and E. H. Adelson. The design and use of steerable filters. *IEEE Trans. on Pattern Analysis and Machine Intelligence*, 13(9):891–906, Sep. 1991.
- [7] H. Gao. M.sc. research proposal: Improved algorithms for tracking fast moving objects. University of Canterbury, 2005.
- [8] W. Geisler. Motion streaks provide a spatial code for motion direction. *NATURE*, 1999.
- [9] R. C. Gonzalez and R. C. Woods. *Digital Image Processing*. Addison-Wesley Publ. Co., 1992.

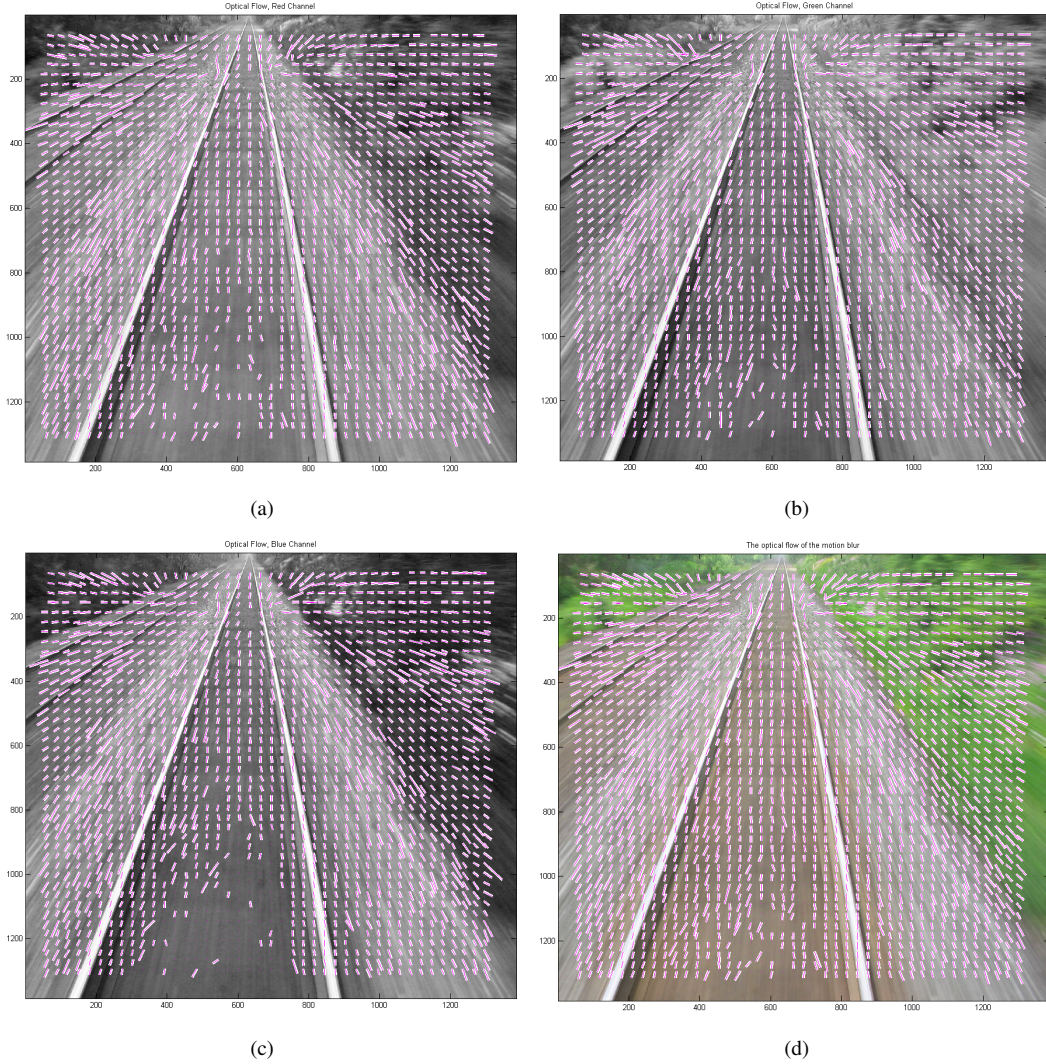


**Figure 5. (a) Optical flow from red channel. (b) Optical flow from green channel. (c) Optical flow from blue channel. (d) Optical flow from combining information from the three color channels.**

- [10] T. Harrington and M. Harrington. Perception of motion using blur pattern information in the moderate and high velocity domains of vision. In *Acta Psychologica*, pages 48:227–237, 1981.
- [11] M. Herman and T. Hong. Visual navigation using optical flow. In *In Proc. NATO Defense Research Group Seminar on Robotics in the Battlefield*, pages 1–9, Paris, France, March 1991. NATO.
- [12] B. Horn and B. Schunck. Determining optical flow. Technical report, Massachusetts Institute of Technology, 1980.
- [13] S. Kawamura, K. Kondo, Y. Konishi, and H. Ishigaki. Estimation of motion using motion blur for tracking vision system. In *Proceedings of the 5th Biannual World Automation Congress*, volume 13, pages 371 – 376, 9-13 June 2002.
- [14] H. Lin and K. Li. Motion blur removal and its application to vehicle speed detection. *Int. Conf. on Image Processing, (ICIP)*, 5(4):3407–3410, October 2004.
- [15] B. D. Lucas and T. Kanade. An iterative image registration technique with an application to stereo vision. In *Proc. of Imaging understanding workshop*, pages 121–130, 1981.
- [16] H. A. Mallot, H. H. Bulthoff, J. Little, and S. Bohrer. Inverse perspective mapping simplifies optical flow computation and obstacle detection. *Biological Cybernetics*, 64:177–185, 1991.
- [17] J. G. Proakis and D. G. Manolakis. *Digital Signal Processing*. Macmillan Publ. Co., second edition, 1992.
- [18] X. Y. Qi, L. Zhang, and C. L. Tan. Motion deblurring for optical character recognition. *8th Int. Conf. on Document Analysis and Recognition (ICDAR)*, pages 389–393, 2005.
- [19] I. Rekleitis. Motion estimation based on motion blur interpretation. Master's thesis, McGill University, School of Computer Science, 1995.
- [20] Y. Yitzhaky and N. S. Kopeika. Identification of blur parameters from motion blurred images. *Graphical Models and Image Processing*, 1997.

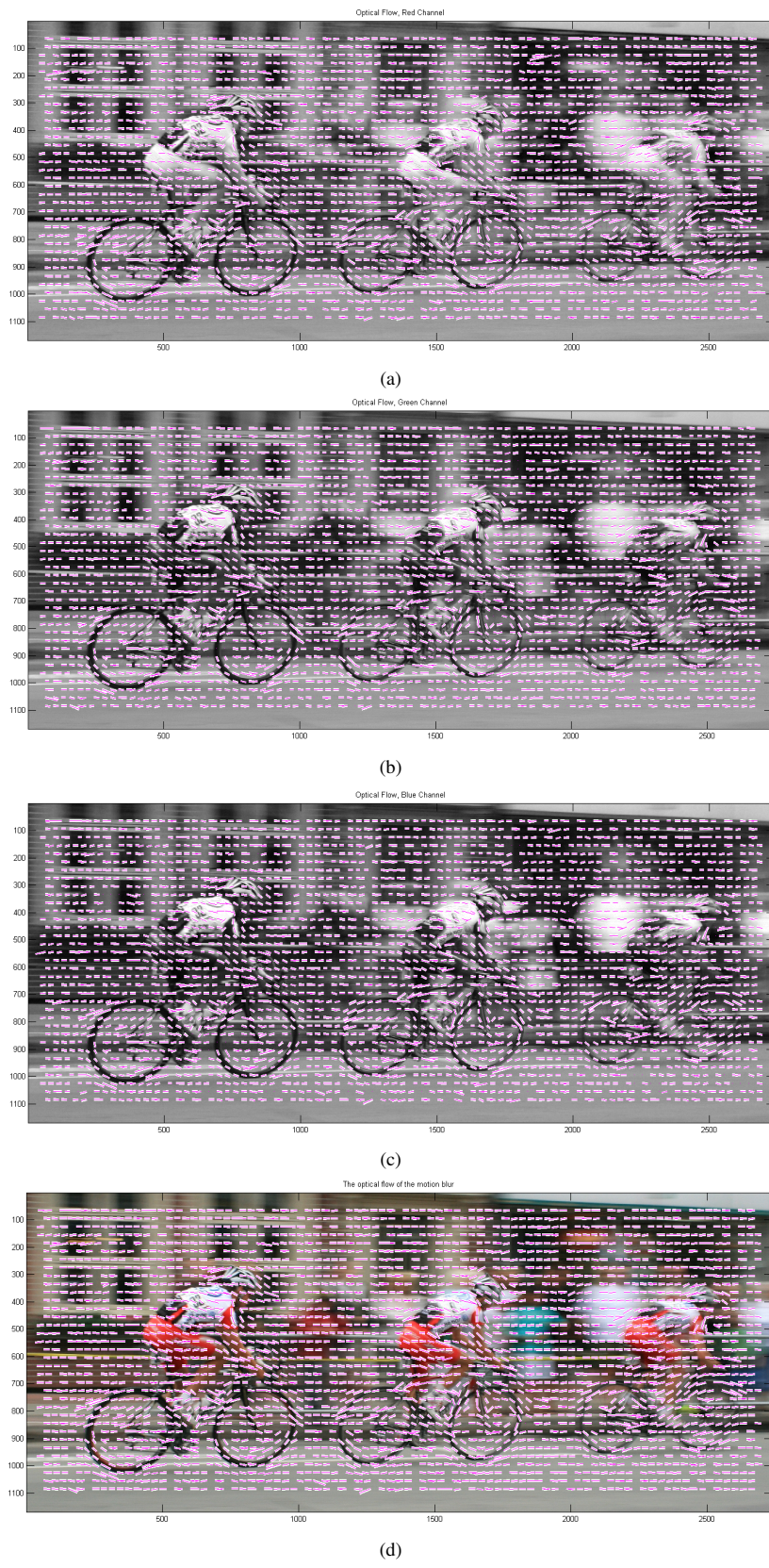


**Figure 6. (a) Optical flow from red channel. (b) Optical flow from green channel. (c) Optical flow from blue channel. (d) Optical flow from combining information from the three color channels.**